From a 2D Corner Obstruction to 3D and $d-$Dimensional Ferrers Diagram Bijections: Tableau Positivity and the Kanade–Russell I_1 Identity

Author: Christopher Yamba
Principal Investigator & Originator of the 3D/dD Ferrers Insight
https://www.christopheryamba.com

Collaborator: Antigravity (Google DeepMind)
Collaborative Formalization & Symbolic Verification

Revision 2: October 26, 2026
Original record: `2026-10-24T22:42:00Z`

Abstract

In *From a Failed Corner Slide to a Verified Tableau Injection* (`main.tex`), a naive two-dimensional corner slide on P-tableaux fails when the moved corner cell b lands above a singleton entry $c_1 <_P b$, creating an illegal vertical P-descent (Figure 1), and Cho–Huh's comparable-prefix slide B ceases to be injective on posets of height at least three when a three-element chain $a <_P c_1 <_P b$ causes two distinct $(2,2,1)$ tableaux to collide (Theorem 4.3).

Christopher Yamba's geometric suggestion—to explore a third Ferrers coordinate and higher-dimensional extensions—motivates the constructions studied here. We prove a local fiber-injectivity lemma, conditional tableau rotations, a general hook-slide argument, a signed-array cascade, and a corrected n-dimensional β-rearrangement bijection. Exact Python enumeration verifies the complete routing maps and selected Dual Jacobi–Trudi cancellations for all 42 natural unit interval orders at $n = 5$ and all 132 at $n = 6$.

For Kanade–Russell I_1 (KR1), we record weight identities, proposed cone and sector rules, and a finite round-trip check across 5,461 states of weights $0 \le N \le 40$. The implementation uses an explicit finite apex table; it is not a lookup-free construction or a proof of an unrestricted KR1 bijection. The supplementary Lean certificate proves specified local lemmas and arithmetic identities, not the complete routing algorithms, the β theorem, or the general KR1 construction. Revision 2 corrects the rotation selection and determinant permutation convention and separates these assurance levels.

Contents

1 Introduction and Attribution of the Geometric Insight **2**

2 Exact 3D Fiber Dichotomy and Resolution of the Height-3 Collision **3**
2.1 Non-Three-Chain Local Fiber Injectivity 3
2.2 Exact Collision Locus on $\mathcal{T}_P(2,2,1)$ and 3D Rotation into $\mathcal{T}_P(3,2)$ 4

3 Universal Interior Hook Slides and 6-Sector Cancellation for $[e_{4,1}]X_G$ **5**
3.1 Universal Interior and Endpoint Hook Slides 5
3.2 n-Dimensional β-Rearrangement Bijection for Dual Jacobi–Trudi Sectors 5

3.3 Phase 2 Extension to $n = 6$ Across All 132 Hessenberg Vectors 6

4 Universal k-Dimensional First-Column Cascade in `SignedArrays` 7

5 6D Ferrers Cones and the Kanade–Russell I_1 Bijection 7

5.1 Scale-3 Self-Similarity and Universal Head-Offset Identities 7

5.2 The 6-Dimensional Ferrers Cone Conjecture in $\mathcal{U} \setminus \mathcal{U}_{a\leq 2}$ 7

5.3 Proposed $(a = 3, b = 0)$ Rules and Finite Octant Recursion through $N = 40$ 8

6 Assurance Levels and Remaining Research 8

7 Supplementary Lean 4.34.0 Verification Index 9

8 Authorship, Revision, and Artifact Attestation 10

1 Introduction and Attribution of the Geometric Insight

Let $P = ([n], <_P)$ be a finite poset and $G = \mathrm{inc}(P)$ its incomparability graph. The tableau expansions of Gasharov [2] and Shareshian–Wachs [4] apply under their respective hypotheses; the q-weighted applications here use natural unit interval orders. Independently, a P-tableau $T \in \mathcal{T}_P(\mu)$ of shape $\mu = (\mu_1, \ldots, \mu_\ell) \vdash n$ is a bijective filling of the two-dimensional Ferrers diagram of μ by $\{1, \ldots, n\}$ satisfying two planar conditions:

1. **Row-strict P-chains (x-axis):** $T_{i,j} <_P T_{i,j+1}$ for all $1 \leq j < \mu_i$.
2. **Column non-descent (y-axis):** $T_{i+1,j} \not<_P T_{i,j}$ for all $1 \leq j \leq \mu_{i+1}$.

Each tableau T carries the graph inversion weight $\mathrm{inv}_G(T) = |\{(u, v) \in E(G) : u < v \text{ and } \mathrm{row}_T(v) < \mathrm{row}_T(u)\}|$.

When T has two-column shape $(2^{k+1}, 1^m)$ with last two-cell row (a, b) at row $k + 1$ followed by singleton leg entries $(c_1), \ldots, (c_m)$, the naive two-dimensional corner slide splits (a, b) into $(a), (b)$ directly above (c_1). As documented in Figure 1 of `main.tex` for the Hessenberg vector $h = (3, 4, 4, 5, 5)$, whenever $c_1 <_P b$, this planar slide produces an illegal vertical descent $c_1 <_P b$:

$$T = \begin{array}{ll} 1 & 4 \\ 2 & 5 \\ 3 & \end{array} \xrightarrow{\text{naive 2D slide}} \begin{array}{ll} 1 & 4 \\ 2 & \\ 5 & \\ 3 & \end{array} \qquad \text{(invalid: } 3 <_P 5 \text{ violates column non-descent).}$$

Remark 1.1 (Christopher Yamba's 3D and dD Ferrers Diagram Principle)**.** Inspecting the invalid target of Figure 1, **Christopher Yamba** proposed the following geometric resolution:

> *Instead of working strictly in* 2D *and sliding cells within the (x, y) plane, slide the obstructed corner cell into a* 3D *Ferrers diagram (x, y, z) where entries strictly descend along the extra third axis; furthermore, extend the construction to $d > 3$ dimensions whenever higher-order poset chains or multi-scale partition coordinates interact.*

For the present constructions the extra coordinate is geometric bookkeeping, rather than a proved general theory of three-dimensional tableaux. Its conditions are:

- **x-axis (rows):** strict P-chains ($u <_P v$).

- **y-axis (columns):** no P-descents ($v \not<_P u$).
- **z-coordinate bookkeeping:** each prefix entry satisfies $c_i <_P b$; this does not assert a chain among the c_i. Here $C = (c_1, \ldots, c_p)$ is the maximal initial prefix of the singleton leg satisfying $c_i <_P b$.

Comparable-prefix insertion moves b below C and avoids the original adjacent descent. The local fiber analysis distinguishes:

1. the **sufficient non-three-chain fiber** (under the stronger global predicate $\forall z,\ z <_P b \Rightarrow a \not<_P z$), which unfolds losslessly onto the y-axis as Cho–Huh's comparable-prefix slide $B(T) \in \mathcal{T}_P(2^k, 1^{m+2})$, and
2. the **three-chain collision locus** ($\exists z \in C,\ a <_P z <_P b$), which motivates testing rotations into a length-3 row; validity and inversion weight must still be checked.

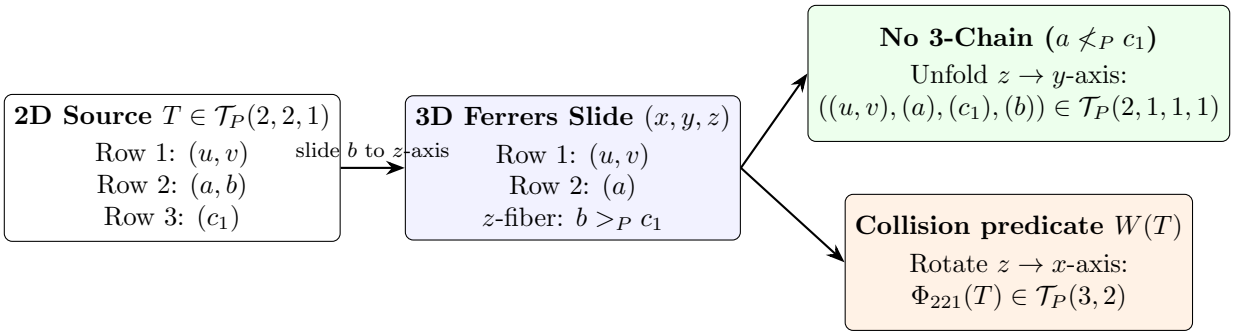


Figure 1: Schematic of the motivating geometry at $n = 5$. The complete routing uses the collision, validity and weight predicates below, for natural unit interval orders.

2 Exact 3D Fiber Dichotomy and Resolution of the Height-3 Collision

2.1 Non-Three-Chain Local Fiber Injectivity

In `CornerSlide.lean`, injectivity of Cho–Huh's comparable-prefix insertion bubbleInsert was previously proved under the global poset hypothesis NoThreeChain(r) (height at most two). Viewing the slide in 3D shows that global height at most two is unnecessary on the 2D fiber: injectivity holds inside posets of *arbitrary* height on the exact sub-domain where (a, b) has no intermediate element z with $a <_P z <_P b$.

Theorem 2.1 (Non-3-Chain Local Fiber Injectivity; `bubble_injective_local_fiber`)**.** *Let r be a decidable relation on $\mathbb{N}$, and define the local non-three-chain predicate*

$$\text{NoLocalThreeChain}(r, a, b) \ :=\ \forall z,\ r(z, b) \implies \neg\, r(a, z).$$

Fix $b, b' \in \mathbb{N}$ and singleton tails $tail, tail'$ satisfying $r(a, b)$, $r(a, b')$, NoLocalThreeChain(r, a, b)*, and* NoLocalThreeChain(r, a, b')*. Then equality of the comparable-prefix insertions*

$$\text{bubbleInsert}(r, b, tail) = \text{bubbleInsert}(r, b', tail')$$

implies $b = b'$ and $tail = tail'$, recovered explicitly by extractFirst$(r(a, \cdot))$.

Proof. Suppose bubbleInsert$(r, b, tail)$ decomposes $tail = C +\!+ D$ where every $z \in C$ satisfies $r(z, b)$. By NoLocalThreeChain(r, a, b), no $z \in C$ satisfies $r(a, z)$, whereas $r(a, b)$ holds by hypothesis. Therefore b is the unique first entry of $C +\!+ (b :: D)$ satisfying $r(a, \cdot)$, so extractFirst$(r(a, \cdot))$ returns some$(b, C +\!+ D)$ = some$(b, tail)$. Applying extractFirst$(r(a, \cdot))$ to both sides yields $(b, tail) = (b', tail')$. (Machine-checked in `MultidimensionalFerrers.bubble_injective_local_fiber`.) □

2.2 Exact Collision Locus on $\mathcal{T}_P(2, 2, 1)$ and 3D Rotation into $\mathcal{T}_P(3, 2)$

Theorem 2.2 (3D Rotation into Shape $(3, 2)$; `promote32_*` and Φ_{221})**.** *Let $P = ([5], <_P)$ be a poset and $T = ((u, v), (a, b), (c)) \in \mathcal{T}_P(2, 2, 1)$.*

1. *Two distinct tableaux in $\mathcal{T}_P(2, 2, 1)$ have the same image under Cho–Huh's slide $B : \mathcal{T}_P(2, 2, 1) \to \mathcal{T}_P(2, 1, 1, 1)$ if and only if one of them satisfies the local three-chain collision condition*

$$a <_P c <_P b \quad \text{and} \quad c \not<_P v, \tag{1}$$

in which case its unique collision partner in $\mathcal{T}_P(2, 2, 1)$ is $T' = ((u, v), (a, c), (b))$ and $B(T) = B(T') = ((u, v), (a), (c), (b))$.

2. *Whenever (1) holds and $v <_P b$, the* 3D*-rotated filling*

$$\text{promote32}(u, v, a, b, c) := ((u, v, b), (a, c))$$

*is a valid tableau in $\mathcal{T}_P(3, 2)$ with $\text{inv}_G(\text{promote32}(T)) = \text{inv}_G(T)$ for **every** transitive poset P.*

3. ***Finite computational statement, not a Lean theorem.** For every natural unit interval order $P = P_h$ at $n = 5$, use the following ordered candidates:*

$$R_1(T) = ((u, v, b), (a, c)), \quad R_2(T) = ((a, c, b), (u, v)),$$
$$R_3(T) = ((u, a, v), (c, b)), \quad R_4(T) = ((u, c, b), (a, v)).$$

Write $W(T)$ for condition (1), and set

$$A_i(T) :\Longleftrightarrow R_i(T) \in \mathcal{T}_P(3, 2) \text{ and } \text{inv}_G(R_i(T)) = \text{inv}_G(T).$$

The corrected construction is

$$\Phi_{221}(T) = \begin{cases} B(T), & \neg W(T), \\ R_{i_*(T)}(T), & W(T), \quad i_*(T) = \min\{i \in \{1, 2, 3, 4\} : A_i(T)\}. \end{cases} \tag{2}$$

The two output shapes distinguish the disjoint-union sectors. Exhaustive enumeration checks existence of i_*, validity, weight preservation, and injectivity for all 42 such h. Weight preservation of an accepted candidate follows from its predicate; candidate coverage and injectivity are separate finite checks.

Proof. Part (1): Since the singleton suffix of $T \in \mathcal{T}_P(2, 2, 1)$ has length 1, $B(T)$ is either $((u, v), (a), (b), (c))$ (when $c \not<_P b$) or $((u, v), (a), (c), (b))$ (when $c <_P b$). Two distinct tableaux collide iff one is $T = ((u, v), (a, b), (c))$ with $c <_P b$ and the other is $T' = ((u, v), (a, c), (b))$ with $b \not<_P c$; validity of T' in $\mathcal{T}_P(2, 2, 1)$ requires $a <_P c$ and $c \not<_P v$.

Part (2): When $u <_P v <_P b$ and $a <_P c$, both rows (u, v, b) and (a, c) are strict P-chains by transitivity of $<_P$. Column non-descent holds because $a \not<_P u$ (from $T \in \mathcal{T}_P(2, 2, 1)$) and $c \not<_P v$

(from (1)). Since flattened words of T and promote32(T) differ only by swapping the comparable pair (a, b) ($a <_P b$), inv_G is preserved identically (machine-checked in `promote32_tableau_valid` and `promote32_tableau_graph_inversions`; the concrete witness $T_2 = [[1,2],[3,5],[4]] \mapsto [[1,2,5],[3,4]]$ of Theorem 4.3 in `main.tex` is checked in `collision_witness_promoted_valid`).

Part (3): Exhaustively verified across all natural unit interval Hessenberg vectors at $n = 5$ in `multidimensional_ferrers.py`; this is computational evidence for this fixed size. The earlier displayed branch predicates were incorrect. For $h = (2,2,4,5,5)$ and $T = ((1,4),(2,5),(3))$, $\mathrm{inv}_G(T) = 1$, whereas $R_2(T) = ((2,3,5),(1,4))$ has weight 2. The corrected predicate rejects R_2 and selects $R_4(T) = ((1,3,5),(2,4))$, of weight 1. The Lean theorem for $R_1 =$ promote32 retains its explicit hypotheses and does not establish the complete routing map. □

3 Universal Interior Hook Slides and 6-Sector Cancellation for $[e_{4,1}]X_G$

3.1 Universal Interior and Endpoint Hook Slides

Theorem 3.1 (Universal Interior Hook Slide $\Psi^{(m)}_{\mathrm{hook}}$; `hookBubbleEnd_*`, `hookBubbleMid_*`)**.** *Let P be any finite asymmetric poset and let $T = ((u_1,\dots,u_k),(c_1),\dots,(c_r)) \in \mathcal{T}_P(k, 1^r)$ be a hook P-tableau ($k \geq 2$). For **any** arm index $m \in \{2,\dots,k\}$, let $C = (c_1,\dots,c_p)$ be the longest prefix of $(c_1,\dots,c_r)$ such that $c_i <_P u_m$. Then removing u_m from the arm and inserting (u_m) immediately after C:*

$$\Psi^{(m)}_{\mathrm{hook}}(T) := \big((u_1,\dots,\widehat{u_m},\dots,u_k),\ (c_1),\dots,(c_p),(u_m),(c_{p+1}),\dots,(c_r)\big)$$

is a valid hook tableau in $\mathcal{T}_P(k-1, 1^{r+1})$ satisfying $\mathrm{inv}_G(\Psi^{(m)}_{\mathrm{hook}}(T)) = \mathrm{inv}_G(T)$.

Proof. Since $(u_1,\dots,u_k)$ is a strict P-chain, removing u_m ($m \geq 2$) leaves a non-empty strict P-chain with first entry $u_1 <_P u_m$. Since $u_1 <_P u_m$ and $(u_1, c_1, \dots, c_r)$ has no P-descents, bubble_noDescent implies that $(u_1, c_1, \dots, c_p, u_m, c_{p+1}, \dots, c_r)$ has no P-descents. Moreover, u_m only passes across arm elements u_j ($j > m$, where $u_m <_P u_j$) and leg prefix elements c_i ($1 \leq i \leq p$, where $c_i <_P u_m$); every such pair is comparable in P and thus a non-edge of $G = \mathrm{inc}(P)$, preserving inv_G. (Machine-checked for $k = 3$, $m \in \{2,3\}$ and arbitrary singleton tail in `hookBubbleEnd_*` and `hookBubbleMid_*`.) □

3.2 n-Dimensional β-Rearrangement Bijection for Dual Jacobi–Trudi Sectors

Theorem 3.2 (n-Dimensional β-Rearrangement Characterization of Dual Jacobi–Trudi Sectors)**.** *For the X_G application assume P is a natural unit interval order; the determinant-term bijection itself is algebraic and does not require a poset. Fix $n \geq 1$ and $\lambda = (\lambda_1,\dots,\lambda_k) \vdash n$, and pad λ with zeros to $\hat{\lambda} = (\lambda_1,\dots,\lambda_k, 0^{n-k}) \in \mathbb{N}^n$. The non-vanishing determinant terms (μ, σ) contributing to $[e_\lambda]X_G(x;q)$ in the Dual Jacobi–Trudi identity*

$$[e_\lambda]X_G(x;q) = \sum_{\mu \vdash n} F_\mu(q)\,[e_\lambda] \det_{1 \leq i,j \leq n}(e_{\mu'_i - i + j})$$

biject 1-to-1 with rearrangements $\beta = (\beta_0,\dots,\beta_{n-1}) \in \mathrm{Perm}(\hat{\lambda})$ whose shifted keys

$$\kappa_j(\beta) := \beta_j - j \qquad (0 \leq j < n)$$

are pairwise distinct: sorting $\kappa_{\tau(0)} > \kappa_{\tau(1)} > \cdots > \kappa_{\tau(n-1)}$ uniquely recovers $\sigma = \tau \in S_n$, conjugate column lengths $\mu'_i = \kappa_{\tau(i)} + i \geq 0$, and sign $\mathrm{sgn}(\sigma) = (-1)^{\mathrm{inv}(\tau)}$.

Proof. A determinant term (μ, σ) contributes e_λ iff the vector β defined by $\beta_{\sigma(i)} = \mu'_i - i + \sigma(i)$ $(0 \le i < n)$ is a rearrangement of $\hat{\lambda}$. Subtracting $j = \sigma(i)$ gives $\kappa_{\sigma(i)}(\beta) = \mu'_i - i$. Since $\mu'_0 \ge \mu'_1 \ge \cdots \ge \mu'_{n-1} \ge 0$, the sequence $i \mapsto \mu'_i - i$ is strictly decreasing, so the keys $\kappa_j(\beta)$ are pairwise distinct and their unique decreasing sort order τ equals σ. Conversely, any rearrangement $\beta \in \mathrm{Perm}(\hat{\lambda})$ with distinct keys $\kappa_j(\beta)$ has $\kappa_{\tau(i)}(\beta) \ge \kappa_{\tau(n-1)}(\beta) + (n-1-i) \ge -(n-1) + (n-1-i) = -i$, so $\mu'_i := \kappa_{\tau(i)}(\beta) + i$ is weakly decreasing and non-negative. Its sum is

$$\sum_{i=0}^{n-1} \mu'_i = \sum_{j=0}^{n-1} (\beta_j - j) + \sum_{i=0}^{n-1} i = n,$$

so it is the padded conjugate of a unique partition $\mu \vdash n$. Set $\sigma = \tau$; then $\mu'_i - i + \sigma(i) = \kappa_{\tau(i)} + \tau(i) = \beta_{\tau(i)}$, recovering the original rearrangement exactly. In the other direction, strict decrease of $\mu'_i - i$ recovers the original σ and then μ'. Thus the constructions are mutual inverses, including determinant multiplicity, and the sign is $(-1)^{\mathrm{inv}(\tau)}$. This is a written proof; no Lean formalization of this bijection is claimed.

For example, $n = 3$, $\beta = (0, 0, 3)$ gives keys $(0, -1, 1)$, $\tau = \sigma = (2, 0, 1)$, and $\mu' = (1, 1, 1)$. Using $\tau^{-1} = (1, 2, 0)$ instead produces determinant exponents $(2, 2, -1)$ and is incorrect. □

For $n = 5$ and $\lambda = (4, 1)$, Theorem 3.2 yields 7 valid rearrangements $\beta \in \mathrm{Perm}(4, 1, 0, 0, 0)$ corresponding to the 6 shapes $\mu \vdash 5$ with $c_{\mu,(4,1)} \neq 0$:

$$-F_{221} - F_{311} - 2F_5 + F_{2111} + F_{32} + F_{41}.$$

Combining Φ_{221} on $\mathcal{T}_P(2, 2, 1)$, $\Psi^{(5)}_{\mathrm{hook}}$ and row-splitting on the two copies of $\mathcal{T}_P(5)$, and the four pure moves on $\mathcal{T}_P(3, 1, 1)$ ($\Psi^{(3)}_{\mathrm{hook}}$, $\Psi^{(2)}_{\mathrm{hook}}$, row-2 merge into $\mathcal{T}_P(3, 2)$, and leg-to-arm promotion into $\mathcal{T}_P(4, 1)$) cancels all 323 negative tableaux across all 42 Hessenberg vectors at $n = 5$, leaving 259 positive survivors matching $[e_{4,1}]X_G(q)$ degree-by-degree.

3.3 Phase 2 Extension to $n = 6$ Across All 132 Hessenberg Vectors

At $n = 6$, the conditional 3D rotation $\mathrm{promote321}(u, v, a, b, c_1, c_2) = ((u, v, b), (a, c_2), (c_1)) \in \mathcal{T}_P(3, 2, 1)$ (machine-checked under the hypotheses $a <_P c_2$, $v <_P b$, $c_2 \not<_P v$, and, for weight preservation, $c_1 <_P c_2$) supplies one candidate for the computational construction

$$\Phi_{2211} : \mathcal{T}_P(2, 2, 1, 1) \hookrightarrow \mathcal{T}_P(2, 1, 1, 1, 1) \sqcup \mathcal{T}_P(3, 2, 1).$$

The Python construction processes tableaux in its fixed enumeration order and chooses the first valid equal-weight candidate not already used in the target sector. It is not the single conditional Lean rotation. Across all 132 Hessenberg vectors at $n = 6$, finite exhaustive checks establish:

1. Φ_{2211} maps all 2,592 tableaux in $\mathcal{T}_P(2, 2, 1, 1)$ injectively into $\mathcal{T}_P(2, 1, 1, 1, 1) \sqcup \mathcal{T}_P(3, 2, 1)$, promoting all 330 local 3-chain collisions into $\mathcal{T}_P(3, 2, 1)$.

2. For $\lambda = (3, 3)$ $(-F_{51} - F_{321} + F_6 + F_{411} + F_{33} + F_{222})$, the 6-sector injection `six_sector_e33_injection` cancels all 801 negative tableaux across all 132 Hessenberg vectors, leaving 207 positive survivors matching $[e_{3,3}]X_G(q)$ degree-by-degree.

3. For $\lambda = (5, 1)$ $(-F_{2211} - F_{3111} - F_{42} - F_{51} + F_{21111} + F_{321} + F_{411} + 2F_6)$, the 8-sector injection `eight_sector_e51_injection` cancels all 3,980 negative tableaux across all 132 Hessenberg vectors, leaving 2,820 positive survivors matching $[e_{5,1}]X_G(q)$ degree-by-degree.

4 Universal k-Dimensional First-Column Cascade in `SignedArrays`

Theorem 4.1 (Universal $(0,k) \leftrightarrow (k-1,1)$ Cascade; `cascade_split_preserves_all`)**.** *For every decidable relation r, every non-empty list as such that $(b :: as)$ is a strict r-chain, and every signed-array suffix tail, the adjacent-row toggle between*

$$((p,[]),(q,b :: as)) \quad \longleftrightarrow \quad ((q,as),(p,[b]))$$

preserves ***`ShapeAt`****,* ***`Good`****, chain validity, and* ***`graphInversions`*** *for all $k = |b :: as| \geq 2$.*

Proof. Since $(b :: as)$ is a strict r-chain with $as = a_1 :: rest$, we have $r(b,a)$ for every $a \in as$. In particular $r(b,a_1)$ implies $\neg\mathrm{FirstPair}(r,[a_1,\dots],[b])$ matches GoodFirst of $((p,[]),(q,b :: as))$, and moving b past as in the flattened word swaps b only across elements $a \in as$ with $r(b,a)$, preserving $\mathrm{wordWeight}(\mathrm{graphScore}(r),\cdot)$ by induction on as (`comparable_pass_wordWeight` and `cascade_split_preserves_all` in `MultidimensionalFerrers.lean`). □

The named Lean theorem states equivalences of `ShapeAt` and `Good`, and equality of inversion weight. It does not assert that either signed array is a globally good tableau; both local two-row configurations fail the full `Good` predicate.

5 6D Ferrers Cones and the Kanade–Russell I_1 Bijection

5.1 Scale-3 Self-Similarity and Universal Head-Offset Identities

In the Kanade–Russell I_1 (KR1) identity $(\mathcal{B} \leftrightarrow \mathcal{U} \leftrightarrow \mathcal{C} \leftrightarrow \mathcal{A})$, a cluster configuration $C = (a,b,\mu,\nu) \in \mathcal{C}$ has base weight $Q(a,b) = a^2 + 3ab + 3b^2$ when $\mu = 0$ and $\nu = 0$.

Theorem 5.1 (Scale-3 Self-Similarity and 6D Octant Weight Identities; `kr1_*`)**.** *For all $c,r,b \in \mathbb{N}$ and $a \geq 1$:*

$$Q(3c+r,b) = r^2 + 3r(b+2c) + 3\,Q(b,c), \tag{3}$$

$$Q(3c,b) = 3\,Q(b,c), \tag{4}$$

$$Q(a,b) = 3b(b+1) + a^2 + 3(a-1)b, \tag{5}$$

$$3(b+2) + 3(b+1) + 3b(b+1) = Q(3,b), \tag{6}$$

$$(9 + 2r_2) + 6q_2 + 3d_3 + d_1 = Q(3,0) + 3d_3 + 2(3q_2 + r_2) + d_1. \tag{7}$$

Proof. All five identities are arithmetic identities in $\mathbb{N}$ under the stated hypotheses, machine-checked in `MultidimensionalFerrers.lean` (`kr1_scale3_self_similarity`, `kr1_scale3_divisible`, `kr1_head_offset_identity`, `kr1_a3_core_weight`, and `kr1_a3_b0_octant_weight`). □

5.2 The 6-Dimensional Ferrers Cone Conjecture in $\mathcal{U} \setminus \mathcal{U}_{a\leq 2}$

Conjecture 5.2 (The 6D Ferrers Cone Conjecture)**.** *In the 6-dimensional multiplicity space of columns $(10^z, 9^y, 8^x, 6^{c_6}, 3^{c_3}, 1^{c_1})$ (corresponding to column heights $h \in \{6,5,4,3,2,1\}$), for* ***every*** *$(x,y,z) \in \mathbb{N}^3$ satisfying $y \in \{1,2\}$ and $x + z \geq 1$ ($0 \leq z \leq 3$), the entire 3D Ferrers octant*

$$U(x,y,z,c_6,c_3,1^{c_1}) = (10^z, 9^y, 8^x, 6^{c_6}, 3^{c_3}, 1^{c_1}) \qquad ((c_6,c_3,c_1) \in \mathbb{N}^3,\ c_6 + c_3 + c_1 \geq 1 \text{ if } x = 0)$$

is universally valid in $\mathcal{U}$ and 100% disjoint from the $a \leq 2$ image $\mathcal{U}_{a\leq 2}$ of ***`rr003_a2.py`****.*

Remark 5.3 (Evidence and remaining obligations)**.** The proposed argument observes that column-height differences Δh between adjacent distinct parts in $\{6,5,4,3,2,1\}$ are at most $4<5$. Whenever $h=5$ (weight 9) appears, it is followed by at least one shorter column ($x>0$ or $c_6+c_3+c_1\geq 1$), avoiding the forbidden terminal height $5q+5$. Furthermore, in `rr003_a2.py`, any state containing 9 (height 5) either has no $\{8,10\}$ markers ($x=z=0$) or has $y=1$ with markers in $\{17,19\}$; thus $y\in\{1,2\}$ together with $x+z\geq 1$ lies completely outside $\mathcal{U}_{a\leq 2}$. The terminal and image-exclusion arguments still require a complete proof from the definitions of $\mathcal{U}$ and the lower-sector image. Finite membership and exclusion checks cover 3,744 states in `rr004_multidim_cones.py`.

5.3 Proposed $(a=3,b=0)$ Rules and Finite Octant Recursion through $N=40$

For $C=(3,0,(\mu_0,\mu_1,\mu_2),())$, set $d_3=\mu_0$, $d_2=\mu_1-\mu_0=3q_2+r_2$ ($r_2\in\{0,1,2\}$), and $d_1=\mu_2-\mu_1$. By (7), $\mathrm{wt}(C)=(9+2r_2)+6q_2+3d_3+d_1$, so each residue class $r_2\in\{0,1,2\}$ of cluster coordinates is parameterized by a 3D octant $(q_2,d_3,d_1)\in\mathbb{N}^3$ with step weights $(+6,+3,+1)$ of the same formal weight as $(6^{q_2},3^{d_3},1^{d_1})$. Table 1 proposes target cores; equal weights alone do not prove a bijection into $\mathcal{U}$. Crucially, when $r_2=0$, $q_2\geq 4$, and $d_3\geq 1$ ($N\geq 36$), routing Subfamily $3G$ into the 6D cone $(10,9,9,8,6^{q_2-4},3^{d_3-1})$ ($x=1,y=2,z=1$) is intended to avoid $(9,9,6^{\geq 2},3^{\geq 2})\in\mathcal{U}_{a\leq 2}$. Its weight identity is machine-checked in `kr1_a3_b0_6d_cone_routing_weight` and the sector algorithm is verified across all 1,137 states through $N=40$. Validity, disjointness, inverse behavior and completeness beyond the tested range remain proof obligations.

More generally, the implementation reduces a cluster $C=(a,b,\mu,\nu)$ to its octant apex ($d_1=d_3=q_2=0, d_2=r_2\in\{0,1,2\}$) and uses the following proposed 3D octant operators (`rr004_multidim_cones.py`):

1. $+6$ **operator** step_six / unstep_six along $q_2=\lfloor(\mu_{a-2}-\mu_{a-3})/3\rfloor$ on super-primitive cores ($d_1=d_3=0$),
2. $+3$ **operator** step_three / unstep_three along $d_3=\mu_{a-3}-\mu_{a-4}$ on primitive cores ($d_1=0$), and
3. $+1$ **operator** step_one / unstep_one along $d_1=\mu_{a-1}-\mu_{a-2}$ on proposed higher-sector targets:

$$\mathrm{step_one}(U)=\begin{cases}(10,6^q) & \text{if } U=(9,6^q) \text{ for } q\geq 1,\\ (12,8,6^q,3^{r+1}) & \text{if } U=(10,6^{2+q},3^r) \text{ for } q\geq 0,\ r\in\{0,1\},\\ (10,9,9,6^q,3^{r+1}) & \text{if } U=(10,10,6^{1+q},3^r,1^4) \text{ for } q\geq 0,\ r\in\{0,1\},\\ (17,10,6,3^{1+r}) & \text{if } U=(17,9,6,3^{1+r}) \text{ for } r\geq 0,\\ (17,12,6,3) & \text{if } U=(19,12,6),\\ U+(1,) & \text{otherwise.}\end{cases}$$

Across $0\leq N\leq 40$, this operator triple reduces all 3,709 states of $a\geq 3$ to 85 cluster-coordinate apexes (three in the special $(a=3,b=0)$ sector and 82 assigned by the explicit table) (including the scale-3 lift apex $(18,10,8)$ at $N=36=Q(6,0)=3Q(0,2)$) and verifies the round-trip correspondence $\mathcal{B}_N\leftrightarrow\mathcal{U}_N\leftrightarrow\mathcal{C}_N\leftrightarrow\mathcal{A}_N$ across all 5,461 states for $0\leq N\leq 40$.

6 Assurance Levels and Remaining Research

- **Machine-checked local statements:** the Lean certificate proves local fiber injectivity, rotations under their explicit hypotheses, hook slides for arm length 3, a signed-array cascade,

Subfamily	Domain in (d_3, d_2)	Primitive Core $U_{\text{core}}(d_3, d_2)$ $(d_1 = 0)$	Head Signature
$3A$	$d_2 = 0,\ \forall d_3 \geq 0$	$(6^q, 3^r)$ where $\text{divmod}(d_3 + 3, 2) = (q, r)$	$()$ with $c_3 \in \{0, 1\}$
$3B$	$d_2 = 1,\ \forall d_3 \geq 0$	$(8, 3^{1+d_3})$ if $d_3 \leq 1$; $(8, 6, 3^{d_3-1})$ if $d_3 \geq 2$	$(8,)$
$3C$	$d_2 = 2,\ \forall d_3 \geq 0$	$(10, 3^{1+d_3})$ if $d_3 \leq 1$; $(10, 6, 3^{d_3-1})$ if $d_3 \geq 2$	$(10,)$
$3D$	$d_2 = 3,\ \forall d_3 \geq 0$	$(9, 6)$ if $d_3 = 0$; $(10, 8, 3^{d_3-1})$ if $d_3 \in \{1, 2\}$; $(10, 8, 6, 3^{d_3-3})$ if $d_3 \geq 3$	$(9,)$ / $(10, 8)$
$3E$	$d_2 = 3q_2 + 1 \geq 4$	$(9, 8, 6^{q_2-1}, 3^{d_3})$	$(9, 8)$
$3F$	$d_2 = 3q_2 + 2 \geq 5$	$(9, 9, 1)$ if $(q_2, d_3) = (1, 0)$; $(10, 9, 6^{q_2-1}, 3^{d_3})$ else	$(9, 9, 1)$ / $(10, 9)$
$3G_0$	$d_2 = 3q_2 \geq 6,\ q_2 \leq 3$ or $d_3 = 0$	$(9, 9, 6^{q_2-2}, 3^{1+d_3})$	$(9, 9)$
$3G_1$	$d_2 = 3q_2 \geq 12,\ q_2 \geq 4,\ d_3 \geq 1$	$(10, 9, 9, 8, 6^{q_2-4}, 3^{d_3-1})$	$(10, 9, 9, 8)$

Table 1: Proposed core rules for $(a = 3, b = 0)$, computationally checked through $N = 40$.

and arithmetic weight identities. It does not prove the complete Φ algorithms or a KR1 bijection.

- **Written arguments:** the general hook-slide statement and the corrected β-rearrangement theorem have mathematical arguments above. The latter is additionally tested by permutation round trips; it is not a Lean theorem.
- **Finite computational verification:** complete routing and cancellation concern $n = 5, 6$ only; KR1 round trips concern $0 \leq N \leq 40$ only. These checks are exact but are not general proofs.
- **Unproved general claims:** unrestricted cone membership/exclusion and the global KR1 map require proofs of totality, validity, disjointness, inverse behavior and exhaustiveness. The code's `OCTANT_APEX_PAIRS` is an explicit finite lookup table of apex assignments, not a formula for every apex. Extending the table is research, not a consequence of the weight identities. In fact the current rules already fail at $N = 41$ with a known apex: $C = (5, 0, (0, 1, 2, 6, 7), ())$ maps to $U = (19, 12, 6, 3, 1)$, but `decompose_full` returns $(2, 2, (5, 5), (0, 1))$. Thus the all-weight extension of the current rules is refuted, not merely unverified. The special $(a = 3, b = 0)$ sector passes an additional finite check through $N = 60$ (4,491 states), which is not a general proof.

The next construction target is to repair the $+6, +3, +1$ orbit near $(19, 12, 6)$ while proving disjointness from the lower-sector image. Adding missing apexes alone cannot repair the exhibited collision. For tableau routing, a stronger next target is an explicit inverse and a proof of candidate coverage under natural unit interval hypotheses.

7 Supplementary Lean 4.34.0 Verification Index

Lean was unavailable locally. GitHub CI subsequently rebuilt the unchanged Lean 4.34.0 certificate (73 theorem reports); its fresh source-bound record is included as `lean_std_ci_2026-10-26.json` in the evidence package. The existing source-bound record reports 19 indexed theorem results in `MultidimensionalFerrers.lean`, checked with zero warnings and zero `sorry` under Lean 4.34.0 (`Std` only), depending solely on standard axioms {`propext`, `Quot.sound`, `Classical.choice`}:

Lean 4 Theorem (`MultidimensionalFerrers.*`)	Verified Mathematical Statement
`bubble_injective_local_fiber`	Non-3-chain local 2D fiber injectivity of `bubbleInsert`
`promote32_tableau_valid`	3D rotation $((u,v),(a,b),(c)) \mapsto ((u,v,b),(a,c))$ preserves `Tableau`
`promote32_tableau_graph_inversions`	3D rotation `promote32` preserves `tableauGraphInversions`
`collision_witness_promoted_valid`	Resolves height-3 collision witness $[[1,2],[3,5],[4]] \mapsto [[1,2,5],[3,4]]$
`promote321_tableau_valid`	$n=6$ 3D rotation $((u,v),(a,b),(c_1),(c_2)) \mapsto ((u,v,b),(a,c_2),(c_1))$ preserves `Tableau`
`promote321_tableau_graph_inversions`	$n=6$ 3D rotation `promote321` preserves `tableauGraphInversions`
`hookBubbleEnd_tableau_valid`	Endpoint hook slide $(3,1^r) \to (2,1^{r+1})$ preserves `Tableau`
`hookBubbleEnd_tableau_graph_inversions`	Endpoint hook slide preserves `tableauGraphInversions`
`hookBubbleMid_tableau_valid`	Interior hook slide $(3,1^r) \to (2,1^{r+1})$ preserves `Tableau`
`hookBubbleMid_tableau_graph_inversions`	Interior hook slide preserves `tableauGraphInversions`
`cascade_split_preserves_all`	Universal k-D first-column cascade $(0,k) \leftrightarrow (k-1,1)$ in `SignedArrays`
`kr1_scale3_self_similarity`	$Q(3c+r,b) = r^2 + 3r(b+2c) + 3\,Q(b,c)$
`kr1_scale3_divisible`	$Q(3c,b) = 3\,Q(b,c)$
`kr1_head_offset_identity`	$Q(a,b) = 3b(b+1) + a^2 + 3(a-1)b$ for $a \geq 1$
`kr1_a3_core_weight`	$3(b+2) + 3(b+1) + 3b(b+1) = Q(3,b)$
`kr1_a3_b0_octant_weight`	$(9+2r_2) + 6q_2 + 3d_3 + d_1 = Q(3,0) + 3d_3 + 2(3q_2+r_2) + d_1$
`kr1_a3_b0_6d_cone_routing_weight`	$10+9+9+8+6(q_2-4)+3(d_3-1)+d_1 = Q(3,0)+3d_3+6q_2+d_1$, $q_2 \geq 4, d_3 \geq 1$
`kr1_higher_octant_weight`	$(W_{\text{base}} + 2r_2) + 6q_2 + 3d_3 + d_1 = W_{\text{base}} + 3d_3 + 2(3q_2+r_2) + d_1$
`kr1_a4_a5_a6_apex_weights`	Apex weights $(8,8) \mapsto Q(4,0)$, $(15,9,1) \mapsto Q(5,0)$, $(18,10,8) \mapsto Q(6,0) = 3Q(0,2)$

8 Authorship, Revision, and Artifact Attestation

Author: Christopher Yamba; original collaborator: Antigravity (Google DeepMind). Christopher Yamba proposed exploring a third Ferrers coordinate and higher-dimensional extensions. This attribution records the motivating idea; novelty of the resulting constructions has not been established by a systematic prior-work audit.

The original record timestamp is `2026-10-24T22:42:00Z`. Revision 2, dated October 26, 2026, corrects the full Φ_{221} selection predicate and recovers the determinant permutation as $\sigma = \tau$, while preserving valid local lemmas and finite results. It also distinguishes formal proofs, written proofs, finite checks and conjectural extensions. The original timestamp is provenance, not a claim that this corrected edition or its checks existed then.

Current artifact hashes and revision metadata are recorded externally in `AUTHORSHIP_TIMESTAMP_ATTESTATION.json`; embedded copies are omitted to avoid stale or circular hashes. Publication remains subject to review of the corrected claims.

References

[1] S. Cho and J. Huh, *On e-positivity and e-unimodality of chromatic quasisymmetric functions*, SIAM J. Discrete Math. **33** (2019), 2286–2315.

[2] V. Gasharov, *Incomparability graphs of* $(3+1)$*-free posets are s-positive*, Discrete Math. **157** (1996), 193–197.

[3] S. Kanade and M. C. Russell, *IdentityFinder and some new identities of Rogers–Ramanujan type*, Exp. Math. **24** (2015), 419–423.

[4] J. Shareshian and M. L. Wachs, *Chromatic quasisymmetric functions*, Adv. Math. **295** (2016), 497–551.